2892

Influence of Modulation Instability on Brillouin-based Distributed Optical Fiber Sensors

M. Alahbabi, P. Wait*, Y. Cho, A. Hartog* and T. P. Newson

Optoelectronics Research Centre, University of Southampton

Southampton, SO17 1BJ, United Kingdom

Tel: +44 23 8059 3836 Fax: +44 23 8059 3149

mna@orc.soton.ac.uk

*Sensa, Gamma House, Enterprise Road, Chilworth Science Park, Southampton, SO167NS, UK.

Abstract: The performance of Brillouin based distributed fiber sensors is largely determined by the peak power governed by non-linear thresholds that can be launched into the sensing fiber. Our investigations show that in long-range (>20km) sensors using standard single mode fiber operating at 1.5μm, modulation instability can limit the acceptable pulse power to below 100mW. Using NZ-DSF with negative dispersion avoids this problem and allows a seven-fold increase in launch power.

OCIS codes: *060.2370, 290.1350, 290.5830, 060.4370*

1. INTRODUCTION

Long range Brillouin-based distributed optical fiber sensors attract a lot of interest due to their potential usage for monitoring temperature/strain of underground power cables, live optical links and large scale structures. Brillouin frequency shift and the change in its intensity may be used to simultaneously spatially resolve temperature and strain change along the sensing length [1]. Whilst some groups have focused on ultra-high spatial resolution in short range sensors [2], our research has focused on

maximizing the sensing range and improving the sensor's accuracy at long distance. A necessary requirement of our technique is that the launched probe pulse power is limited to below the threshold of any non-linear effects that would otherwise introduce errors in the detected Brillouin signal. We have identified that in long range sensors, using standard single mode fibers (SMF), operating at 1.5μm, modulation instability (MI) has the lowest threshold.

MI is the process by which a cw beam becomes unstable due to the interaction between the non-linearity and anomalous dispersion in the fiber. This instability induces spectral sidebands situated symmetrically around the pump signal which grow with power and distance along the fiber [3, 4].

In distributed temperature and strain sensors based on spatially resolving the frequency and intensity of the spontaneous backscattered anti-Stokes Brillouin signal along the sensing length, these sidebands are detrimental to the measurement. The Brillouin back-scattered signal is typically about 11GHz from the probe frequency and Rayleigh scattering, from the MI induced sidebands, overlap the Brillouin signal and prevent accurate determination of the latter's intensity. MI is only present in anomalous dispersion fiber and so by using Non-Zero Dispersion Shifted Fiber NZ-DSF (MetroCor) with negative dispersion at 1.5μm, this limitation is overcome and much higher probe power can be used.

2. MODULATION INSTABILITY

Analysis of the non-linear Schrödinger Equation for anomalous loss less fiber yields the following key results [5]: The gain at a frequency ω from the pump frequency is given by

$$G(\omega) = |\beta_2 \omega| \sqrt{(\omega_c^2 - \omega^2)} \qquad (1)$$

The gain exists for $|\omega| \ \omega_c$ where

$$\omega_c^2 = \frac{4\gamma P_0}{|\beta_2|} \qquad (2)$$

P_0 is the input power, β_2 is the fiber dispersion, and γ is the non-linear parameter respectively [6]. The gain is maximized at two frequencies given by:

$$\omega_{\max} = \pm\frac{\omega_c}{\sqrt{2}} = \pm\left(\frac{2\gamma P_o}{|\beta_2|}\right)^{\frac{1}{2}} \qquad (3)$$

By substituting (3) in (1), the maximum gain becomes $G_{(max)}=2\gamma P_0$ where the peak gain is independent of β_2 and increases linearly with the incident power. Figure 1 shows the gain spectra for several values of P_0.

The MI gain spectrum changes along the fiber as a result of fiber loss and pump power depletion[7]. Pump power depletion can generally be neglected unless the sidebands are strongly seeded and the gain profile along the fiber is determined by the local pump power that decreases with distance. When fiber loss is taken into account, the previously calculated critical frequency ω_c, is replaced by $\omega_c \exp(-\alpha L/2)$ where α is the attenuation factor and L is the fiber length. As a result ω_c varies along the fiber length eventually decreases to 0 as the fiber length goes to infinity [5, 8]. Using the expressions provided by Hasegawa *et al.* [6], we have computed the spatially integrated gain and the critical frequency along standard SMF, figure 2.

The critical frequency decreases as the fiber length is increased or the launch power is decreased. For a fiber length of 20km, the critical frequency is approximately 50GHz for a launch power of 400mW and the integrated gain is ~29 dB. Clearly MI can cause broadening of the back-scattered Rayleigh signal and contamination of the detected Brillouin signal when operating in the anomalous dispersion regime. This contamination is seen as an upwards drift in the "Brillouin" signal along the fiber and translates to an upward drift in temperature along the fiber. This paper investigates experimentally the effects of MI on Brillouin-based sensors and demonstrates a useful increase in permissible launch signal power when dispersion shifted fiber with negative dispersion is utilized.

3. EXPERMENTAL DETAILS

MI effects were investigated and compared using SMF and MetroCor fiber. The characteristics of each fiber are summarized in table 1. MI was first demonstrated, using a DFB source at 1533nm, line width 10MHz. A series of power spectra was measured at the output end of 20km

for each fiber as function of the input peak power. The influence of MI on the detected Brillouin backscattered trace was then measured in the SMF and finally distributed temperature measurements using both fibers were performed, using the principle of Brillouin Optical Time-Domain Reflectometry and direct detection of the intensity of the Brillouin signal over a distance of 20km. In both cases, the majority of the selected fiber was maintained at room temperature and a few hundred meters of the fiber was placed in an oven and heated to 60°C. Both the intensity of Brillouin and Rayleigh signals along the sensing fibers were measured with 2^{15} averages and 10m of spatial resolution. Brillouin signal was then divided by the Rayleigh signal to account for the splice and fiber loss. Using the previously determined value of Brillouin intensity change with respect to temperature change ($0.35\%°C^{-1}$) [1], the apparent temperature profiles along the sensing fiber at different input powers were derived and plotted.

4. RESULTS AND DISCUSSION

Figure 3 a & b show the output spectra recorded at the far end of the sensing fiber as the input launch power is increased. Figure 3a is for SMF and figure 3b for the MetroCor fiber. In figure 3a, the MI effect becomes more pronounced as the power increases. Figure 3b demonstrates the expected absence of MI in the MetroCor fiber, due to its negative dispersion at 1.5μm and suggests that larger input powers can be safely used.

To calculate the MI gain in the SMF, the measured power spectra were normalized by the source spectrum, which was also measured at the far end of the fiber but at a low input power where the MI effect is negligible. The results are shown in figure 4 and demonstrate the expected characteristic and distinct sidebands. The measured values of the peak MI gain and critical frequency from figure 4 are summarized in table 2 and compared to the theoretical values

computed for figure 2. The small differences between the theoretical and measured values are within the experimental errors of the measurements.

Figure 5 shows the back-scattered Brillouin Stokes and Anti-Stokes spectrum detected at the front end of the SMF for different input pulse powers. The two largest peaks correspond to the Brillouin signal. The adjacent peaks are due to Rayleigh scattering from the MI spectrally broadened probe. Although the peaks of the MI gain do not coincide with the Brillouin peaks, there is sufficient overlap for the measured Brillouin Stoke and anti-Stokes to be contaminated by the Rayleigh scattering from the broadened probe signal.

Figure 6a shows how this contamination translates to a drift in the measured temperature along the fiber. The effect is more marked as the launch probe power is increased and is only circumvented by limiting the probe power to around 100mW for a 20km sensing length of SMF. At 400mW pulse power, a temperature error of only a few degrees is observed up to about 8km but then increases rapidly to more than 250C at 16km. MetroCor fiber (figure 6b) showed a lower temperature error at the front end of the fiber and no evidence of MI induced drift in the temperature measurement along the entire 20km sensing fiber even when power was increased up to 400mW. The inset indicates the heated section at 10km along the fiber and confirmed that the MetroCor fiber showed a similar Brillouin intensity change with respect to temperature (0.35%/°C) as SMF.

As well as the spatial drift in temperature measurement, the contamination of the Brillouin signal with Rayleigh scattering also produces an increase in the RMS noise in temperature resolution primarily due to the presence of coherent Rayleigh noise. Figure 7 compares the RMS temperature resolution as a function of distance for the two fibers. The RMS value was calculated over 500m every 2km along the entire sensing length. Figure 7 shows that the RMS temperature error in SMF is higher and increased rapidly with distance (e.g. at 18km the temperature resolution was ~52°C), whereas there is just a small deterioration in performance with distance using the MetroCor fiber (e.g. temperature resolution at 18km was ~4°C),

following the expected attenuation (0.4dB/Km) of back-scattered signal due to fiber attenuation. In the MetroCor fiber we found that the input power could be increased up to ~700mW before Stimulated Raman Scattering was observed.

5. CONCLUSION

An investigation was conducted to evaluate MI influence on Brillouin-based distributed sensors. Prior to this study, non-linear effects seen in Brillouin sensors, namely the spatial drift in temperature along the fiber, were initially attributed to exceeding the stimulated Raman scattering threshold. However, due to the absence of any observed Raman signal at the end of the sensing fiber, it was thought that Self-Phase Modulation was responsible. These results now show that MI is responsible for this drift. Using NZ-DSF with negative dispersion at 1.5μm avoids MI and allows probe pulse powers to be increased from around 100mW to up 700mW for sensing lengths of 20km. We conclude that using NZ-DSF allows improved performance of long range, high performance Brillouin-based distributed sensors.

Acknowledgement

We would like to thank Corning Optical Plc and Fiber Core Plc for providing fiber. The authors would also like to acknowledge the helpful consultation with Professor Keith Blow (Aston University), who initially suggested our observed non-linear effects may be due to Modulation Instability.

References:

1. S. M. Maughan, H. H. Kee, and T. P. Newson, *Simultaneous distributed fiber temperature and strain sensor using microwave coherent detection of spontaneous Brillouin backscatter.* Measurement Science & Technology, 2001. **12**(7): p. 834-842.
2. K. Hotate, *Distributed Brillouin Strain Sensing With 1-cm Spatial Resolution by Correlation-Based Continuous-Wave Technique.* IEEE Photonics Technology Letters, 2002. **14**(2): p. 179-181.
3. G. P. Agrawal, *Modulation Instability Induced by Cross-Phase Modulation.* Physical Review Letters, 1987. **59**(8): p. 880-883.
4. S. B. Cavalcanti, et al., *Modulation Instability in the Region of Minimum Group-velocity Dispersion of Single-mode Optical via an Extended Nonlinear Schrödinger Equation.* Physical Review A, 1991. **43**(11): p. 6162-6165.
5. G. P. Agrawal, *Non Linear Fiber Optics*. 1995: Academic Press.
6. A. Hasegawa and K. Tai, *Effects of Modulational Instability on Coherent Transmission Systems.* Optics Letters, 1989. **14**(10): p. 512-513.
7. M. Karlsson, *Modulational Instability in Lossy Optical s.* Optics Letters, 1995. **12**(11): p. 2071-2077.
8. D. Anderson and M. Lisak, *Modulational Instability of Coherent Optical- Transmission Signals.* Optics Letters, 1984. **9**(10): p. 468-470.

Table 1. Characteristics of the compared fibers.

Fiber types	**Fiber Loss** ***(dB/km)***	**Effective Area** $(\mu m)^2$	**Dispersion @1533.2nm** ***ps/(km.nm)***
SMF	*0.20*	*~60*	*+17*
MetroCor	*0.25*	*~50*	*-1.384*

Table 2. The theoretical and measured MI gain and critical frequency in SMF.

Input Power	Theoretical Values		Measured Values	
P_0(mW)	G_{max}(dB)	f_c (GHz)	G_{max}(dB)	f_c (GHz)
400	29	50	30	49
300	22	43	21	39
200	15	35	17	33

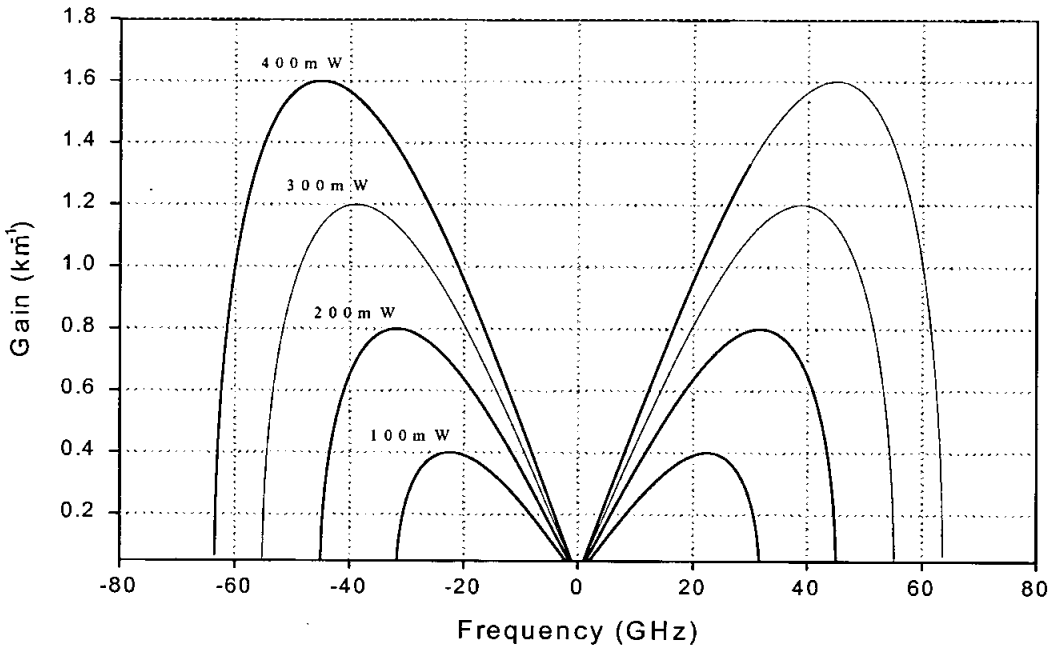

Fig. 1. Gain spectrum of MI versus input power. Parameters: $\beta_2 = -20ps^2/km$ and $\gamma=2(Wkm)^{-1}$ @ 1550nm. After Agrawal [5].

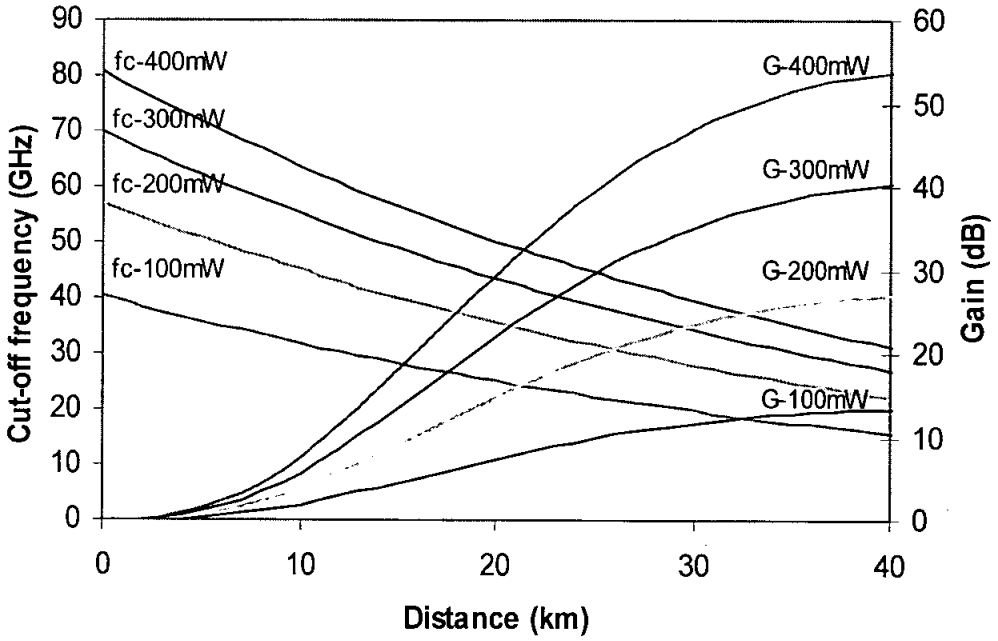

Fig. 2. Spatially integrated gain (right side) and critical frequency (left side) along standard single mode fiber versus input power.

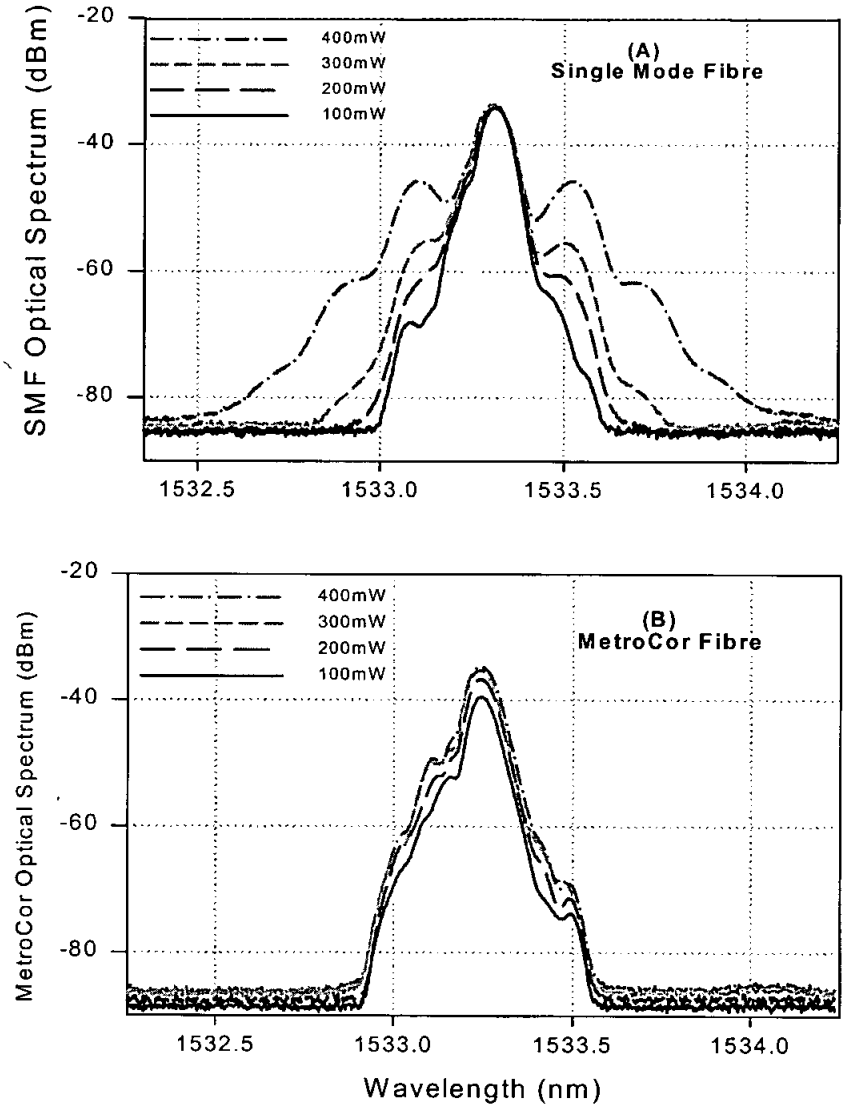

Fig. 3. a & b Power spectra at different peak power at the output end of (a) the SMF (b) MetroCor fiber respectively.

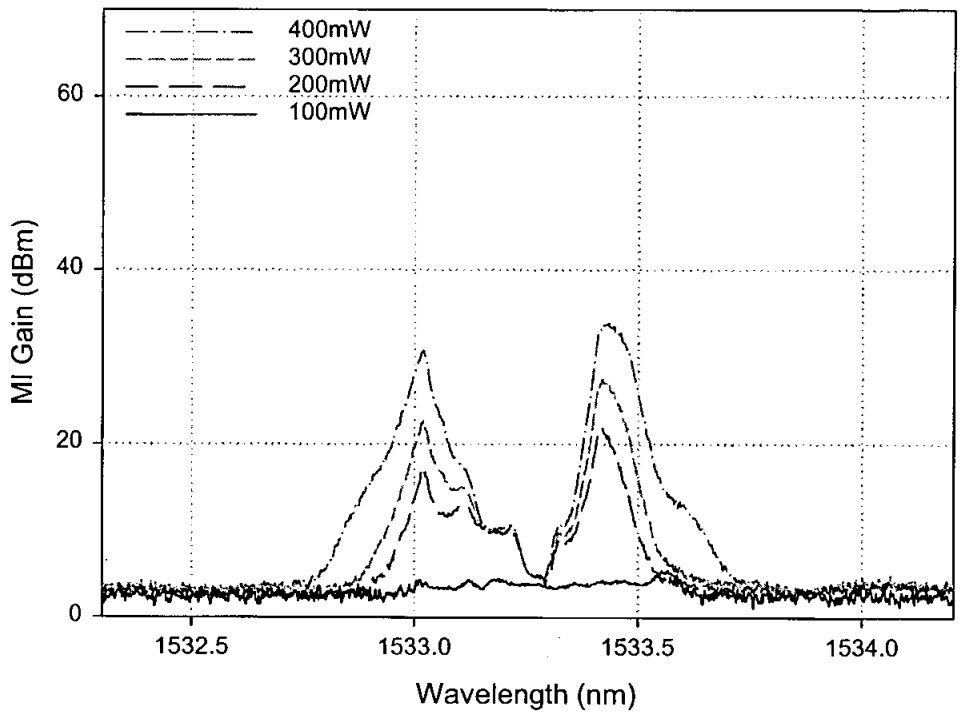

Fig. 4. Measured MI gain and frequency at the output end of 20km of SMF.

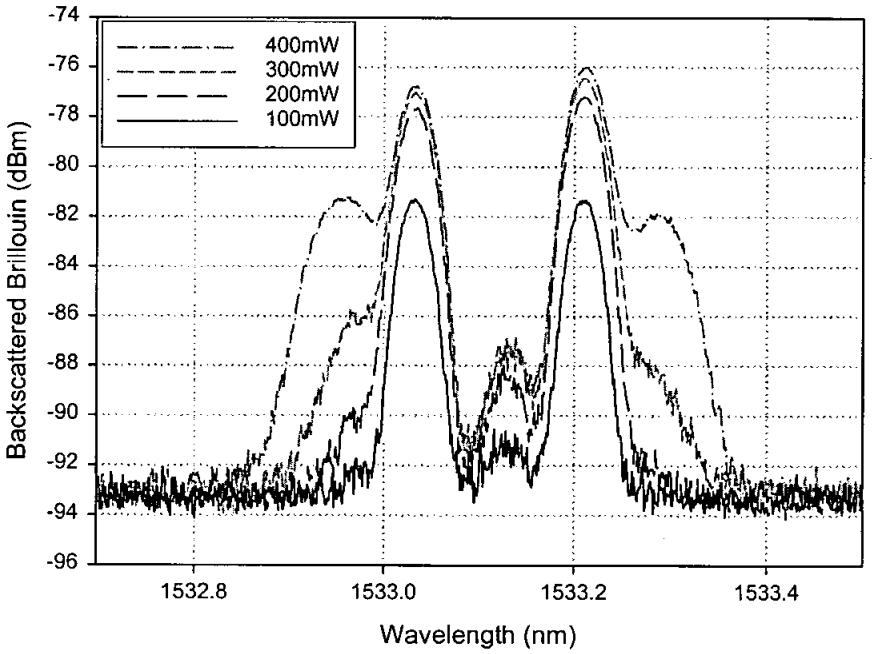

Fig. 5. Brillouin Stokes and Anti-Stokes backscattered spectrum measured at the front end of the fiber for various input power.

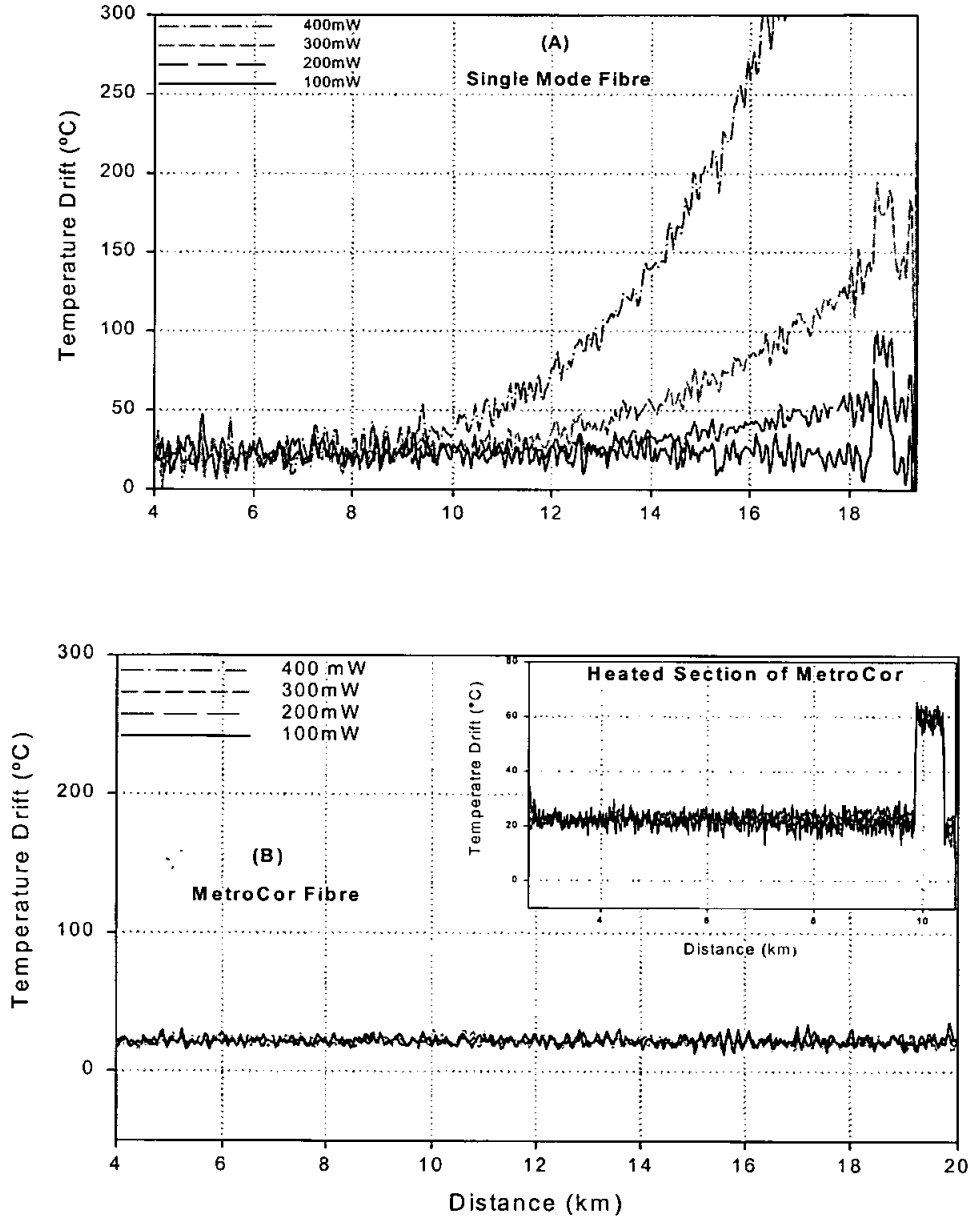

Fig. 6. a & b Temperature drift along (a) 20km of SMF, (b) 20km of MetroCor fiber for various launched power. The inner plot in (b) represents the heated section 10km along the MetroCor fiber.

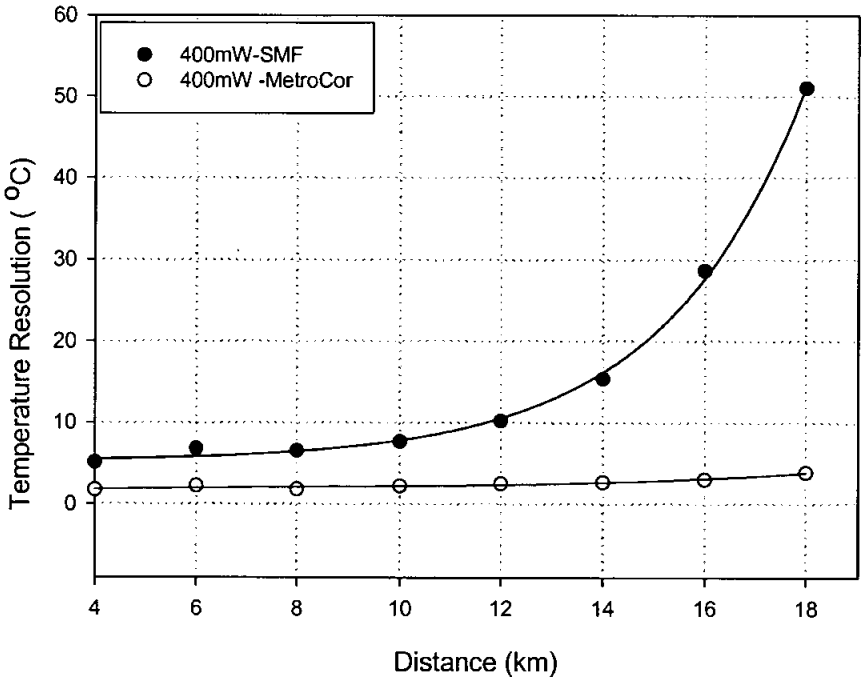

Fig. 7. RMS temperature errors along the characterized sensing fibers at 400mW launched power.